# Gd(III)[15-Metallacrown-5] Recognition of Chiral α-Amino Acid Analogues

Choong-Sun Lim, Joseph Jankolovits, Peng Zhao, Jeff W. Kampf, and Vincent L. Pecoraro*

Department of Chemistry, University of Michigan, Ann Arbor, 930 N. University Ave, Ann Arbor, Michigan 48109, United States

Ⓢ *Supporting Information*

ABSTRACT: Chiral Ln(III)[15-metallacrown-5] complexes with phenyl side chains have been shown to encapsulate aromatic carboxylates reversibly in their hydrophobic cavities. Given the importance of selective guest binding for applications of supramolecular containers in synthesis, separations, and materials design, the affinity of Gd(III)[15-metallacrown$_{Cu(II),\ L-pheHA}$-5] hosts for a series of chiral carboxylate guests with varying substitutions on the α-carbon (phenylalanine, *N*-acetyl-phenylalanine, phenyllactate, mandelate, methoxyphenylacetate) has been investigated. Differential binding of *S*- and *R*-phenylalanine was revealed by X-ray crystallography, as the *S*-enantiomer exclusively forms associative hydrogen bonds with oxygen atoms in the metallacrown ring. Selective guest binding in solution was assessed with isothermal titration calorimetry, which measures the sequential guest binding in the hydrophobic cavity first and the hydrophilic face of the host, and a cyclic voltammetry assay, which quantifies guest binding strength in the hydrophobic cavity of the host exclusively. In solution, the Gd(III)[15-metallacrown$_{Cu(II),\ L-pheHA}$-5] hydrophobic cavity exhibits modest chiral selectivity for enantiomers of phenylalanine (K_S/K_R = 2.4) and mandelate (K_S/K_R = 1.22). Weak binding constants of ~100 M^{-1} were measured for neutral and −1 charged carboxylates with hydrophilic functional groups (ammonium, *N*-acetyl, methyl ether). Weaker binding relative to the unsubstituted guests is attributed to unfavorable interactions between the hydrophilic functionalities of the guest and the hydrophobic cavity of the host. In contrast, binding constants greater than 2000 M^{-1} were measured for α-hydroxy analogues phenyllactate and mandelate. The significantly increased affinity likely arises from the guests being bound as a −2 anion upon metal-assisted deprotonation in the Gd(III)[15-metallacrown$_{Cu(II),\ L-pheHA}$-5] cavity. It is established that guest binding affinity in the hydrophobic cavity of the host follows the general trend of neutral zwitterion < monoanion < dianion, with hydrophilic functional groups decreasing the binding affinity. These results have broad implications for the development of metallacrowns as supramolecular catalysts or in chiral separations.
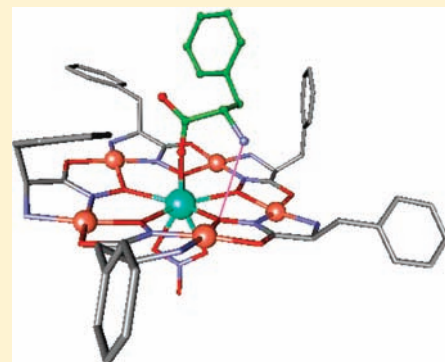
■ INTRODUCTION

Molecular recognition phenomena have widespread implications in catalysis, sensing, molecular storage, and materials design. Reports of supramolecular containers that perform supramolecular catalysis or separate compounds have spurred interest in understanding the interactions between molecular hosts and their guests.[1−7] Fundamentally, thorough characterization of host−guest recognition can provide strategies for overcoming major challenges in supramolecular chemistry, such as chiral recognition[8−11] and achieving turnover in supramolecular catalysis.[4,12] In protic solvents, hydrophobic interactions are a significant driving force for the inclusion of a neutral guest in a supramolecular host. For the encapsulation of anionic species in protic media, charged hosts are typically required to overcome the anion's strong interactions with the solvent.[13,14] Therefore, hosts that combine exposed-metal sites and a hydrophobic pocket have attracted significant interest for anion recognition in protic solvents.[15−23]

Metallacrowns (MCs) are a class of anion recognition agents that often contain numerous open metal-sites in a planar construct.[24−41] For example, Ln(III)[15-MC-5] complexes arrange six metal ions in a 59 Å^2 area that can coordinate anions.[42−49] A hydrophobic cavity can be introduced over one face of the planar Ln(III)[15-MC-5] by incorporating phenylalanine hydroxamic acid (pheHA) ligands. The molecular recognition behavior of Ln(III)[15-MC$_{Cu(II),\ L-pheHA}$-5] complexes (Figure 1a) has been well characterized in the solid-state. Depending on the anion, diverse architectures have been observed, including *p* and *m* helices,[50−52] monomeric complexes,[53−55] octametallacrown cages that assemble into mesoporous solids,[56] and dimeric hydrophobic compartments that sequester a wide variety of guests.[55,57−59] Work has shown that the height of these latter compartments is dependent on the encapsulated anion and its bridging mode between the two MCs in the dimer. As an example, encapsulated isonicotinate guests bind to Cu(II) ring metals via their pyridyl-nitrogen and to the Gd(III) central metal through their carboxylate, generating a 10.29 Å tall compartment.[59] Terephthalate bridges two Gd(III) ions, yielding an 11.89 Å compartment.[58] Even larger guests can fully disrupt compartment formation.[58,60]
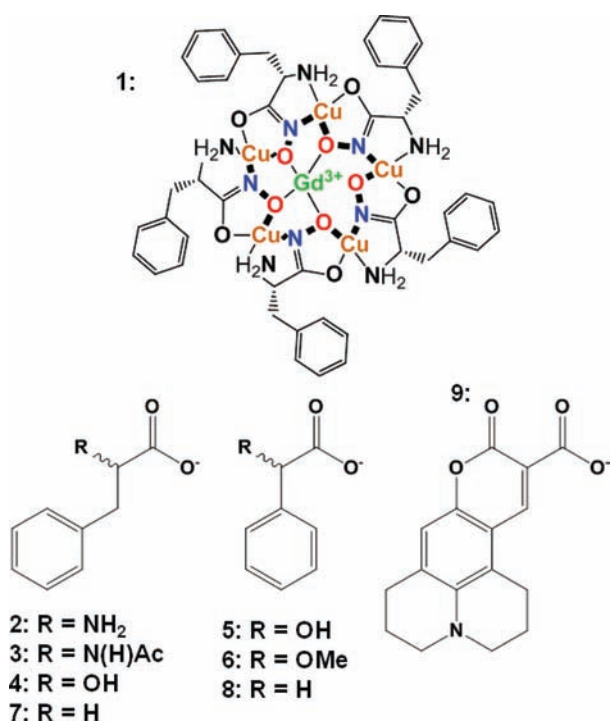
Figure 1. Chemdraw diagrams of Gd(III)[15-MC$_{Cu(II),\ L\text{-}pheHA}$-5] (**1**) and carboxylate guests: *R/S*-phenylalanine (**2**), *N*-acetyl-*R/S*-phenylalanine (**3**), *R/S*-phenyllactate (**4**), *R/S*-mandelate (**5**), *R/S*-methoxyphenyl-acetate (**6**), hydrocinnamate (**7**), phenylacetate (**8**), coumarin 343 (**9**).

While a reasonable understanding of the solid state chemistry of Ln(III)[15-MC$_{Cu(II),\ pheHA}$-5] molecular containers has been developed over the past decade, characterization of the solution behavior of these systems has lagged behind, which can partially be attributed to their paramagnetism obfuscating ^{1}H NMR characterization. Reports have demonstrated that Ln(III)[15-MC$_{Cu(II),\ pheHA}$-5] are stable in aqueous and polar solvents.[45,61] In the past two years, studies have been published that employed fluorescence spectroscopy,[54] isothermal titration calorimetry (ITC),[53] and electrochemical assays[55] to assess anion binding affinities. Guest binding strength increases with more Lewis-acidic lanthanides, implicating the central metal as the primary binding site. Additionally, guests were differentially recognized based on the substitution of the carboxylate. In particular, the less basic benzoate ($K = 447 \pm 32$ M^{-1}) has a much greater affinity for Eu(III)[15-MC$_{Cu(II),\ pheHA}$-5] than the more basic acetate ($K = 115 \pm 17$ M^{-1}),[54] suggesting that guest binding occurs in the hydrophobic pocket. Electrospray ionization mass spectrometry has also revealed monomeric (1:1 and 1:2) MC-guest species with monocarboxylates, while monomeric and dimeric (2:2) MC-guest species have also been detected with dicarboxylate guests.[60] While these initial studies have examined the affinity of Ln(III)[15-MC$_{Cu(II),\ pheHA}$-5] complexes for simple carboxylates, there have been no systematic studies that quantitatively assess how various functional groups influence guest affinity. Furthermore, no studies have attempted to exploit the inherent chirality of the MC to discriminate between chiral guests.

The MC ring in Ln(III)[15-MC$_{Cu(II),\ L\text{-}pheHA}$-5] complexes has the potential to introduce novel molecular recognition capabilities. In a typical hydrophobic cavitand, the inclusion of a hydrophilic substituent would incur a strong energetic penalty. However, Ln(III)[15-MC$_{Cu(II),\ L\text{-}pheHA}$-5] complexes could have favorable interactions with hydrophilic substituents because of associative interactions with the metallic ring. This hypothesis is supported by the observation of hydrophilic solvent molecules bound to the Cu(II) ring metals on the hydrophobic face of MCs in the solid state. Second, the MC face is chiral in the rotational sense of the ring and through the resolved stereocenter on L-pheHA. Because of the stability of the Ln(III)[15-MC-5][45,61,62] and the arrangement of ligands in the MC ring,[48] the host persists as a single diastereomer and does not racemize. Chiral hosts often exhibit enantioselective guest binding,[63−70] which has implications for their use in enantioselective supramolecular catalysts or chiral separations. Given the widespread use of chiral compounds in pharmaceutics, nonlinear optics, and other aspects of materials science, enantioselective synthesis and separations are important research areas. The asymmetric guest binding site on Ln(III)[15-MC$_{Cu(II),\ L\text{-}pheHA}$-5] complexes should be capable of discriminating between enantiomers based on how the guest interacts with the MC ring.

To establish how the guest affinity of Ln(III)[15-MC$_{Cu(II),\ L\text{-}pheHA}$-5] hosts varies based on guest functional groups and chirality, we have investigated the inclusion of phenylalanine (**2**) and related chiral carboxylate guests that differ in the functional group at the α-carbon. (Figure 1, guests **3**−**6**). Comparison of these analogues will allow for preliminary assessment of how factors such as charge, hydrophilicity, and sterics influence guest binding. These guests contain structural features that contribute to guest binding in Ln(III)[15-MC$_{Cu(II),\ L\text{-}pheHA}$-5] hosts, namely, a phenyl ring which engages in associative hydrophobic interactions with the pheHA side chains and a carboxylate which preferentially binds to the central lanthanide ion. We have focused on Gd(III)[15-MC$_{Cu(II),\ L\text{-}pheHA}$-5] hosts (**1**), which display strong guest binding and typically contain an 8-coordinate Gd(III). Herein, we present the first quantitative and structural assessment of chiral guest recognition by chiral Ln-(III)[15-MC$_{Cu(II),\ L\text{-}pheHA}$-5] hosts using single-crystal X-ray diffraction, ITC, and cyclic voltammetry (CV). These experiments reveal a modest preference for the *S*-enantiomer of phenylalanine (**2**) and mandelate (**5**) and a strong thermodynamic preference for α-hydroxy carboxylates. Such selective guest binding has implications for the development of Ln(III)-[15-metallacrown-5] molecular containers in supramolecular catalysts, separation processes, or materials design.

■ EXPERIMENTAL SECTION

All chemicals were used as received. **1**-NO$_3$,[45] **1**-Cl,[54] and sodium ferrocene carboxylate[55] were prepared as previously described. Sodium salts of phenylalanine were prepared by neutralization with sodium hydroxide. Sodium salts of the remaining guests were prepared by neutralization with an equivalent of sodium bicarbonate and stored in a vacuum desiccator over phosphorus pentoxide.

[Gd(III)(S-phe)[15-MC$_{Cu(II)N(L\text{-}pheHA)}$−5](NO$_3$)$_3$] (1-S-2). **1**-NO$_3$ (0.15 mg, 0.1 mmol) was dissolved in 30 mL of water. *S*-**2** sodium salt (0.056 g, 0.3 mmol) was dissolved in 10 mL of water. The solutions were combined, and the product was crystallized upon slow evaporation of the solvent. Yield = 0.141 g, 76%. Analysis for [(C$_{45}$H$_{50}$N$_{10}$O$_{10}$Cu$_5$Gd)(NO$_3$)$_3$(C$_9$H$_{11}$NO$_2$)(H$_2$O)$_8$], found (calcd): C = 36.27 (34.87), H = 4.16 (4.18), N = 9.86 (10.55). ESI-MS gave [(C$_{45}$H$_{50}$N$_{10}$O$_{10}$Cu$_5$Gd)(C$_9$H$_{11}$NO$_2$)(NO$_3$)]$^+$ 1591.3 *m/z*.

Gd(III)(R-phe)[15-MC$_{Cu(II)N(L\text{-}pheHA)}$−5](NO$_3$)$_3$] (1-R-2). **1**-NO$_3$ (0.15 mg, 0.1 mmol) was dissolved in 30 mL of water. *R*-**2** sodium salt (0.056 g, 0.3 mmol) was dissolved in 10 mL of water. The solutions were combined, and the mixture was slowly evaporated to yield single crystals.

Yield = 0.107 g, 57%. Analysis for $[(C_{45}H_{50}N_{10}O_{10}Cu_5Gd)(NO_3)_3\text{-}(C_9H_{11}NO_2)(H_2O)_9]$, found (calcd): C = 36.09 (34.54), H = 4.25 (4.24), N = 9.76 (10.45). ESI-MS gave $[(C_{45}H_{50}N_{10}O_{10}Cu_5Gd)(C_9H_{11}NO_2)(NO_3)]^+$ 1591.3 m/z.

ITC Titrations. Titrations were performed on a VP-ITC from MicroCal, LLC in a 2 mM pH 7.6 aqueous MOPS buffer solution at 293 K. The ITC sample cell was filled with a 0.46 mM **1**-Cl or a 0.47 mM **1**-NO$_3$ solution. Sodium salts of either R-**2** or S-**2** were titrated as ∼140 mM solutions. Reference data on the heats of dilution for each compound were measured in control titrations and subtracted from the reaction data prior to curve fitting analysis to isolate the heat of host–guest complex formation. The data was fit using a sequential binding site (2 binding) model with Origin software. The first titration point was removed from the data fitting. Each titration was repeated at least three times. Thermodynamic parameters were averaged over at least three titration experiments, and the error is reported as the standard deviation.

Cyclic Voltammetry. CV measurements were performed with a BASi Epsilon potentiostat. The working electrode was a 0.0707 cm^2 glassy carbon disk that was polished with 0.05 μm alumina on velvet, rinsed, and sonicated in distilled deionized water prior to each scan. A Pt wire counter electrode and aqueous Ag/AgCl reference electrode (BASi) were employed. The electrochemical cell was water jacketed and held at a constant temperature of 25.0 ± 0.1 °C with a VWR 1145 refrigerated constant temperature controller. *It should be noted that strict temperature control (less than 1 °C variation) is required for accurate competition titration experiments.* The cell was protected from light with a blackout cloth to prevent FcC$^-$ decomposition.[71] No evidence for decomposition was observed through the course of the experiments. CVs were taken with a scan rate of 200 mV/s. Measurements were performed at a ^s_spH of 7.5 in 10 mL of a 0.1 M KCl solution containing 50% methanol, 50% 0.1 M aqueous MOPS buffer solution.[72−74] At this pH the carboxylic acids are deprotonated,[75,76] and MOPS is an effective buffer.[77] The pH was measured with a glass electrode calibrated in aqueous solutions and corrected using the reported constant.[72] No significant changes in the pH were observed through the course of the experiments. The ferrocence carboxylate (FcC$^-$) concentration was 0.6 mM, and the concentration of **1**-Cl was ∼3.2 mM. Prior to the experiments, the solution was purged with nitrogen, and the cell was blanketed with nitrogen through the course of the titrations. Titrants were added as a carefully weighed solid up to the end point of the titration or the solubility limit of the guest, with up to 250 equiv per FcC$^-$ being titrated for weakly bound guests. The shift in the observed $E_{1/2}$ with the change in guest concentration was fit with the following equations using Origin to solve for K_{DG}, the dissociation constant between the competitive guest and **1**, where $E_f^{0'}$ is the potential of free FcC$^-$, $E_c^{0'}$ is the observed potential, K_{red} is the association constant of FcC$^-$ to **1**, K_{ox} is the association constant between the oxidized ferrocenium carboxylate and **1**, K_{Dred} is the dissociation constant between FcC$^-$ and **1**, $[FcC^-]_0$ is the total concentration of FcC$^-$ in solution, $[G]_0$ is the total concentration of the competitive guest in solution, and $[MC]_0$ is the concentration of total concentration of **1** in solution. Titrations were performed three times, and the error is reported as the standard deviation. Values for K_{red} and K_{ox} were taken from the literature.[55]

$$E_c^{0'} = E_f^{0'} + \frac{RT}{F}\ln\left(\frac{1 + K_{red}[MC]_f}{1 + K_{ox}[MC]_f}\right)$$

$$[MC]_f = \frac{-a}{3} + \frac{2}{3}\sqrt{(a^2 - 3b)} \cdot \cos\left(\frac{1}{3}\arccos\left(\frac{-2a^3 + 9ab - 27c}{2\sqrt{(a^2-3b)^3}}\right)\right)$$

$$a = K_{Dred} + K_{DG} + [FcC^-]_0 + [G]_0 - [MC]_0$$

$$b = K_{DG}([FcC^-]_0 - [MC]_0) + K_{Dred}([G]_0 - [MC]_0) + K_{Dred} \cdot K_{DG}$$

$$c = -K_{Dred} \cdot K_{DG}[MC]_0$$

X-ray Crystal Structure Determination. A crystal of dimensions 0.16 × 0.15 × 0.06 mm of **1**-S-**2** and a crystal of dimensions 0.54 × 0.36 × 0.22 mm of **1**-R-**2** were mounted on a standard Bruker SMART CCD-based X-ray diffractometer equipped with a LT-2 low temperature device and normal focus Mo-target X-ray tube (λ = 0.71073 Å) operated at 2000 W power (50 kV, 40 mA). The X-ray intensities were measured at 118(2) K for **1**-S-**2** and 123(2) K for **1**-R-**2**; the detector was placed at a distance 4.954 cm from the crystal. A total of 2727 frames for **1**-S-**2** and 3029 for **1**-R-**2** were collected with a scan width of 0.2° in ω and φ with an exposure time of 60 s/frame of **1**-S-**2** and 30 s/frame of **1**-R-**2**. The frames were integrated with the Bruker SAINT software package[78] with a narrow frame algorithm.

The integration of the data of **1**-S-**2** yielded a total of 66765 reflections to a maximum 2θ value of 52.82° of which 14649 were independent and 12496 were greater than $2\sigma(I)$. The final cell constants were based on the xyz centroids of 6902 reflections above $10\sigma(I)$. Analysis of the data showed negligible decay during data collection; the data were processed with SADABS[79] and corrected for absorption. The structure was solved and refined with the Bruker SHELXTL (version 5.10) software package,[80] using the space group $P2_12_12_1$ with Z = 4 for the formula $C_{54}H_{79}N_{14}O_{30}Cu_5Gd$. All non-hydrogen atoms were refined anisotropically with the hydrogens placed in idealized positions. Full matrix least-squares refinement based on F^2 converged at R_1 = 0.0471 and wR^2 = 0.1065 [based on $I > 2\sigma(I)$], R_1 = 0.0627, and wR^2 = 0.1116 for all data.

The integration of the data of **1**-R-**2** yielded a total of 93242 reflections to a maximum 2θ value of 56.66° of which 17765 were independent and 16902 were greater than $2\sigma(I)$. The final cell constants (Table 1) were based on the xyz centroids of 7537 reflections above $10\sigma(I)$. Analysis of the data showed negligible decay during data collection; the data were processed with SADABS and corrected for absorption. The structure was solved and refined with the Bruker SHELXTL (version 5.10) software package, using the space group $P2_12_12_1$ with Z = 4 for the formula $C_{54}H_{79}N_{14}O_{30}Cu_5Gd$. All non-hydrogen atoms were refined anisotropically with the hydrogen placed in idealized positions. Full matrix least-squares refinement based on F^2 converged at R_1 = 0.0297 and wR^2 = 0.0750 [based on $I > 2\sigma(I)$], R_1 = 0.0323 and wR^2 = 0.0763 for all data.

■ RESULTS

Crystals of **1** with S-**2** and R-**2** were obtained by slow evaporation of an aqueous solution (Figures 2 and 3, respectively). Both structures contain an 8-coordinate Gd(III) central metal. On the MC's hydrophilic faces, a nitrate is bound bidentate to the central metal. On the hydrophobic faces in each structure, S- or R-**2** is bound through a single carboxylate oxygen atom to Gd(III). Two additional unbound nitrates balance the +3 charge of **1**, demonstrating that S- and R-**2** are bound as zwitterions. In each structure, the Gd(III) is displaced toward the hydrophilic face, lying 0.26 Å above the oxygen-mean plane in **1**-S-**2**, and 0.23 Å in **1**-R-**2**. Unlike most previous MC complexes, the hydrophobic faces of the two MCs do not associate. Instead, each monomeric host–guest complex packs roughly perpendicular to the other. The MCs interact in the lattice through a pheHA amine that acts as a hydrogen bond donor to the unbound carboxylate oxygen atom on **2**.

The structures differ in the orientation of the ammonium functional group on **2**. For the S-isomer, the ammonium points toward the MC face (Figure 4), associating with a weak hydrogen bond to two ring oxygen atoms (N−O distances = 3.15 Å, 3.30 Å) and a hydroximate nitrogen (N−N distance = 3.2 Å). The other ammonium protons engage in hydrogen bonds with
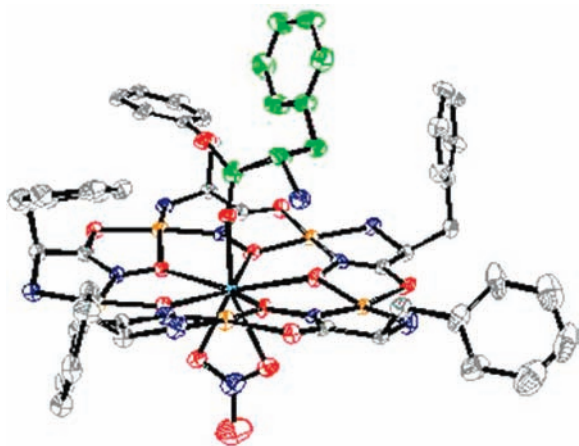
Figure 2. Thermal ellipsoid plot of the crystal structure of **1**-*S*-**2** shown at the 30% probability level. *S*-**2** coordinates to the Gd(III) central metal of **1** through a single carboxylate oxygen atom. The ammonium group on *S*-**2** engages in hydrogen bonding interactions with heteroatoms in the metallacrown ring of **1**. Solvent molecules, hydrogen atoms, and unbound nitrates were removed for clarity. Color scheme: red = oxygen, blue = nitrogen, orange = copper, gray = carbon, turquoise = gadolinium, *S*-**2** carbon = green.
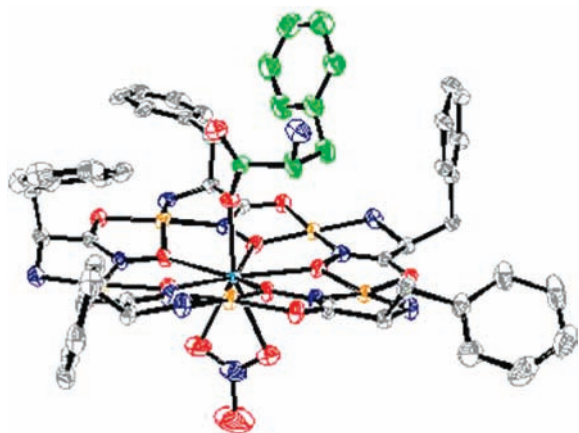
Figure 3. Thermal ellipsoid plot of the crystal structure of **1**-*R*-**2** shown at the 30% probability level. Similar to the coordination mode seen with *S*-**2**, *R*-**2** binds monodentate to the Gd(III) central metal of **1**. The ammonium group on *R*-**2** orients toward the opening in the hydrophobic cavity and does not associate with the MC face. Solvent molecules, hydrogen atoms, and unbound nitrates were removed for clarity. Color scheme: red = oxygen, blue = nitrogen, orange = copper, gray = carbon, turquoise = gadolinium, green = *R*-**2** carbon.

nitrate anions. One forms a 2.82 Å hydrogen bond with a nitrate oxygen that interacts with a Cu(II) ring metal (Cu—O distance = 2.69 Å). The other proton engages in hydrogen bonds with two oxygen atoms on another nitrate (N—O distances of 2.87 Å, 3.10 Å). The unbound carboxylate oxygen atom accepts a hydrogen bond from a water molecule coordinated to a Cu(II) ring metal (O—O distance = 2.80 Å). In the **1**-*R*-**2** structure, the ammonium points away from the MC face and does not interact with the MC (Figure 5). Again, the ammonium acts as a hydrogen bond donor to nitrate anions, with a 2.92 Å hydrogen bond to a nitrate oxygen that forms a 2.80 Å interaction with a Cu(II) ring metal. Another ammonium proton forms two weak
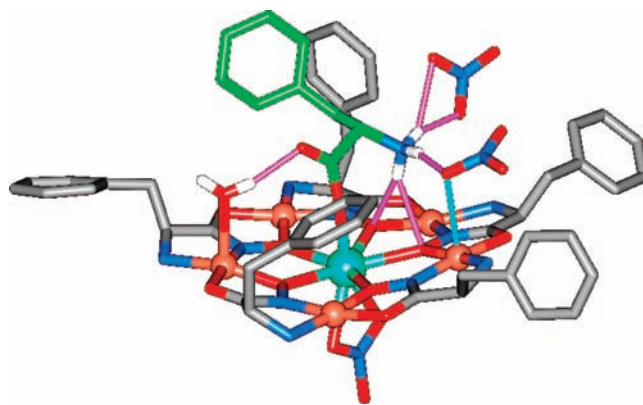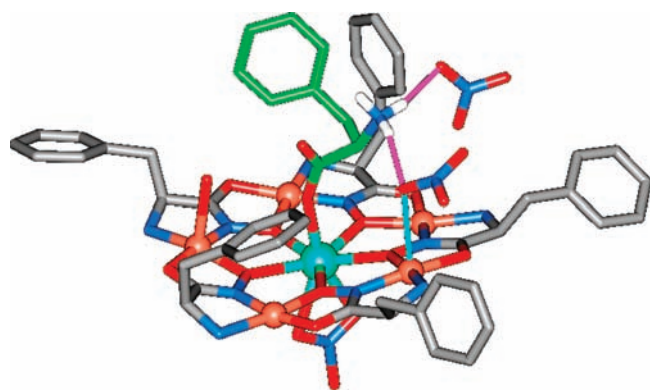

Figure 4. Representation of the X-ray crystal structure of **1**-*S*-**2** that highlights the hydrogen bonding interactions (purple lines) of *S*-**2**. The unbound carboxylate oxygen on *S*-**2** accepts a hydrogen bond from a water coordinated to a Cu(II) ring metal (O—O distance =2.80 Å). The *S*-**2** ammonium acts as a hydrogen bond donor to heteroatoms in the metallacrown ring (N—O distance =3.15, 3.30 Å, N—N distance =3.21 Å), one unbound NO_3^- (N—O distances =2.87, 3.10 Å), and a NO_3^- (N—O = 2.82 Å) that is engaged in a 2.69 Å interaction with a Cu(II) (turquoise line). Remaining solvent molecules and hydrogen atoms were removed for clarity. Color scheme: red = oxygen, blue = nitrogen, orange = copper, gray = carbon atoms on **1**, green = carbon atoms on *S*-**2**, turquoise = gadolinium.

hydrogen bonds with an unbound nitrate, with N—O distances of 3.33 Å and 3.38 Å. The remaining ammonium hydrogen bonds with a pheHA carbonyl oxygen on a proximal MC in the lattice (N—O distance =3.01 Å). A much longer 3.48 Å interaction is observed between the unbound carboxylate oxygen atom on *R*-**2** and a water molecule coordinated to a Cu(II) ring metal. Despite numerous attempts, crystals with guests **3**−**6** bound to **1** were not obtained.

These structures illustrate differential binding of phenylalanine to the metallacrown based upon the chirality of the guest. In particular, the solid state structures suggest preferential binding of the *S*-isomer as it forms an additional hydrogen bond to the metallacrown ring with the pendent ammonium group, whereas the amine of the *R*-isomer orients away from the MC face. However, one must be cautious predicting solution affinity based on crystal structures. In solution, the orientation of the guest in the hydrophobic cavity could easily deviate from the solid state configuration as hydrogen bonding patterns and solvation of the host−guest complexes could differ markedly between the two phases.
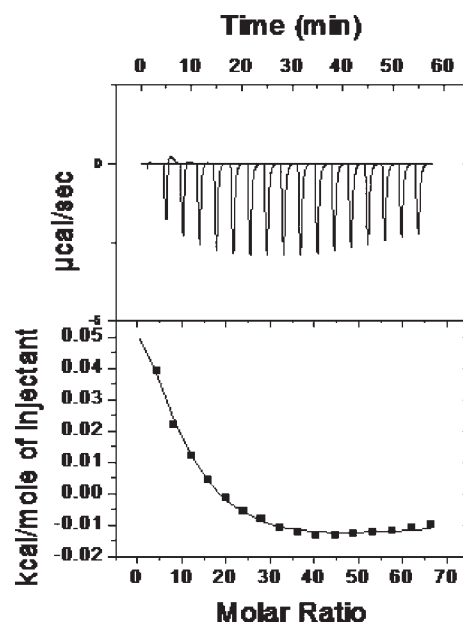
Isothermal titration calorimetry (ITC) and a competitive cyclic voltammetric (CV) assay were utilized to evaluate the extent that the chiral Gd(III)[15-MC$_{L-pheHA}$-5] complex exhibits enantioselective guest recognition in solution. ITC was used to measure the thermodynamics of binding *S*- and *R*-**2** to **1**. ITC data were fit with a sequential two-site binding model. In accordance with the extensive crystallographic characterization of Ln(III)[15-MC-5] host−guest complexes and previously established trends in guest binding affinity,[53−55] the primary binding site is assigned to the hydrophobic cavity of the host, while the second site is assigned to the hydrophilic face. Attempts to fit the data with other models, such as a single-site binding model, resulted in insufficient fits of the experimental data (Supporting Information, Figure 1). ITC titrations (Figure 6) reveal that both enantiomers of **2** bind modestly to **1** with

Figure 5. Representation of the X-ray crystal structure of **1**-*R*-**2** that highlights the hydrogen bonding interactions (purple lines) of *R*-**2**. The *S*-**2** ammonium acts as a hydrogen bond donor to one unbound NO_3^- (N—O distance = 2.83 Å), and a NO_3^- (N—O = 2.92 Å) that is engaged in a 2.72 Å interaction with a Cu(II) (turquoise line). Unlike what was observed in the **1**-*S*-**2** structure, the unbound carboxylate oxygen on *R*-**2** does not hydrogen bond with the water coordinated to the Cu(II) ring metal. Remaining solvent molecules and hydrogen atoms were removed for clarity. Color scheme: red = oxygen, blue = nitrogen, orange = copper, gray = carbon atoms on **1**, green = carbon atoms on *S*-**2**, turquoise = gadolinium.

Figure 6. Isothermal titration calorimetry data corresponding to the titration of *S*-**2** (135.7 mM) into 0.46 mM-**1** at 293 K in 2 mM-MOPS at pH 7.6. The curve was fit with a sequential 2 site binding model.

Table 1. Thermodynamic Parameters for the Binding of 2 to 1-Cl and 1-NO$_3$ Obtained by ITC[a]

	host			
	1-Cl		**1**-NO$_3$	
	guest			
	S-phe	*R*-phe	*S*-phe	*R*-phe
Ka$_1$ (M^{-1})	89 (11)	57 (11)	83 (8)	35 (4)
$\Delta G°_1$ (kcal/mol)	−2.6 (1)	−2.3 (1)	−2.6 (1)	−2.1 (1)
ΔH_1 (kcal/mol)	1.6 (2)	3.2 (4)	2.0 (7)	2.2 (6)
ΔS_1 (cal/mol·K)	14 (1)	19 (2)	16 (2)	15 (2)
Ka$_2$ (M^{-1})	8 (2)	20 (3)	7 (2)	9 (3)
$\Delta G°_2$ (kcal/mol)	−1.2 (2)	−1.7 (1)	−1.1 (1)	−1.3 (2)
ΔH_2 (kcal/mol)	−12 (3)	−4.5 (4)	−15 (3)	−18 (6)
ΔS_2 (cal/mol·K)	−36 (12)	−9 (2)	−47 (10)	−56 (21)

[a] Titrations were performed at 293 K in a 2 mM aqueous MOPS buffer at pH 7.6. The guest was titrated as the sodium salt.

binding constants less than 100 M^{-1} (Table 1, Supporting Information, Tables 1−4). The binding of the first guest is entropy driven, which can be rationalized by a hydrophobic contribution from the release of highly ordered water molecules from the solvation sphere of **2**'s phenyl ring upon its inclusion in the hydrophobic cavity of **1**. In addition, an entropic contribution can arise from bidentate coordination of the carboxylate to Gd(III), which would release two coordinated water molecules. Though this bidentate binding mode is not observed crystallographically for **2**, it is commonly observed for other carboxylate guest. The binding of a second guests is very weak and enthalpy driven, consistent coordination of the carboxylate on the hydrophilic face of the MC, which is typically encountered in the solid state for other guests.

Within experimental error, enantioselectivity was observed between host **1**-Cl (**1** with chloride counterions) and enantiomers of **2**, as a modest thermodynamic preference for *S*-**2** was observed. It is possible that the counterion on **1** could influence guest affinity and the observed enantioselectivity. Crystal structures of Ln(III)[15-MC-5] complexes with chloride show the anion binding exclusively to Cu(II) ring metals on the hydrophilic face, thus it is not expected to effectively compete with carboxylate guests for the host. In contrast, nitrate is frequently observed binding to the central metal, can adopt bidentate coordination modes, and occasionally binds on the hydrophobic face; thus, nitrate is expected to compete with guests for the MC host. Also, nitrate anions influence how *S*- and *R*-**2** are bound to **1** in the solid state by accepting hydrogen bonds from the ammonium on **2**; thus, counterion effects on stereoselectivity seemed possible. To assess the extent of these counterion effects, the binding of **2** to **1**-NO$_3$ was measured for comparison with **1**-Cl; ITC titrations revealed that the magnitude of the binding constants between enantiomers of **2** and **1** were similar with both chloride and nitrate counterions on **1**, suggesting that these anions do not significantly influence guest binding strength. The enthalpic and entropic contributions to the binding strength were also similar. However, **1**-NO$_3$ displays slightly greater enantioselectivity than **1**-Cl.

To characterize enantioselective and chemoselective guest binding to **1** further, the binding strengths of chiral phenylalanine analogues (guests **3**−**6**) were measured. These measurements were performed with CV using our recently reported competitive binding assay.[55] In the assay, ferrocene carboxylate (FcC$^-$) is utilized as a redox probe. The observed $E_{1/2}$ of FcC$^-$ increases in the presence of **1** because FcC$^-$ binding to the cationic host stabilizes the reduced state of the probe. The sodium salts of guests **3**−**6** displace FcC$^-$ from **1**, shifting $E_{1/2}$ back to the value of free FcC$^-$ (Figure 7). The binding strength of the competitive guest can be calculated based on this potential shift using the binding strength of FcC$^-$ to **1**-Cl, which was previously reported.[55] Measurements were performed at ^s_spH of 7.5 in a 0.1 M KCl solution containing 50% methanol, 50% aqueous MOPS solution
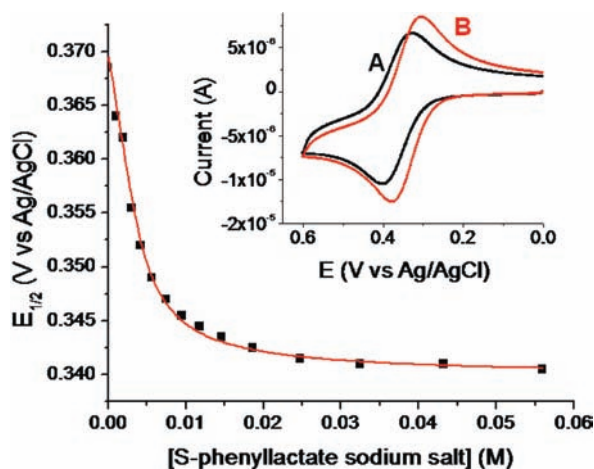
Figure 7. Plot of $E_{1/2}$ vs guest concentration from a CV competition titration of S-4 to 1. The data fitting curve is shown in red. Conditions were 0.6 mM sodium FcC$^-$, 3.4 mM 1-Cl, 100 mM KCl in a 50% methanol 50% 100 mM aq MOPS buffer, $_s^s$pH = 7.5. Inset: CVs of FcC$^-$ in a solution containing A: 5.7 equiv of 1 and B: 5.7 equiv of 1 and 93 equiv of S-4. The observed $E_{1/2}$ for FcC$^-$ shifts to more positive values, relative to the free $E_{1/2}$, upon binding to 1. The addition of S-4 displaces FcC$^-$ from 1, shifting the observed $E_{1/2}$ back toward value for free, unbound FcC$^-$.

(v/v). FcC$^-$ is fully deprotonated under these conditions[75,76] and displays a fully reversible redox wave throughout the titration, as indicated by the ΔE_p and the ratio of the anodic and cathodic peak currents. No potential drift is observed in the reference electrode during the experiments, and the potential of free FcC$^-$ is not affected by the presence of the competitive guest in the absence of 1 or by changes in the ionic strength, indicating that the observed potential shift results entirely from the competitive binding equilibrium. Plots of $E_{1/2}$ versus the concentration of 1 were fit to obtain association constants for guest binding. The CV data were adequately fit with a model where only one guest is bound, which is attributed to the guest binding in the hydrophobic cavity. While the binding of a second guest was detected by ITC, this binding strength is very weak (K_2 = 10−30 M^{-1}). ITC is capable of determining the weak binding of the second guest because it detects complex formation directly by measuring changes in heat. In contrast, the CV assay detects the displacement of the FcC$^-$ probe from the host by a competitive guest. Once FcC$^-$ is displaced from the host, it can no longer detect the binding of a second guest. Thus the indirect detection of guest binding in the competitive binding assay precludes quantification of the thermodynamics of sequential guest binding. Similarly, the binding of a second guest was not observed in a fluorescence competitive binding assay.[54] Furthermore, the high concentration of KCl electrolyte employed in the CV assay could limit guest binding on the hydrophilic face, where chloride has been shown to bind crystallographically.

The association constants between 1-Cl and each enantiomer of guests 3−6 are shown in Table 2. Guests 3 and 6 display modest K_a values of approximately 100 M^{-1} with 1. In contrast, guests 4 and 5 bind much more strongly, with K_a values of over 2000 M^{-1}. 1 only shows statistically significant enantioselectivity toward 5, with a 22% preference for the S-enantiomer. The binding strength of 2 to 1 could not be measured by the CV competitive binding assay because 2 disturbed the potential and reversibility of FcC$^-$ in the absence of 1.

Table 2. Binding Constants for Guests 3−9 to 1

guest	K_a (M^{-1})	ΔG^0 (kcal/mol)
N-acetyl-S-phenylalanine (S-3)[a]	82 ± 16	−2.6 ± 0.2
N-acetyl-R-phenylalanine (R-3)[a]	70 ± 7	−2.5 ± 0.1
S-phenyllactate (S-4)[a]	2070 ± 140	−4.52 ± 0.07
R-phenyllactate (R-4)[a]	2140 ± 110	−4.54 ± 0.05
S-mandelate (S-5)[a]	3260 ± 70	−4.79 ± 0.02
R-mandelate (R-5)[a]	2680 ± 120	−4.67 ± 0.04
S-methoxyphenylacetate (S-6)[a]	140 ± 10	−2.9 ± 0.1
R-methoxyphenylacate (R-6)[a]	120 ± 20	−2.8 ± 0.2
hydrocinnate (7)[b]	370 ± 20	−3.51 ± 0.03
phenylacetate (8)[b]	306 ± 8	−3.39 ± 0.01
coumarin 343 (9)[c]	12,800 ± 300	−5.60 ± 0.02

[a] Values correspond to association constants determined by the competition CV assay. Solution conditions were 100 mM KCl in 10 mL of a 50% methanol 50% 100 mM aq MOPS buffer, $_s^s$pH = 7.5. Reported errors are the standard deviation of three or more titrations. [b] Values correspond to the binding of the first guest as determined by ITC at 298 K in 2 mM aqueous MOPS buffer at pH 7.6.[53] Reported errors are the standard deviation of three or more titrations. [c] Value was determined by fluorescence in 20 mM aqueous hexamethylenetetramine buffer at pH 6.0.[54]

**Table 3. Enantiomeric Discrimination of Various α-Substituted Carboxylate Guests by Host 1**

guest	host	K_S/K_R	p-value[c]
phenylalanine (2)[a]	1-Cl	1.6	0.02
phenylalanine (2)[a]	1-NO$_3$	2.4	0.00043
N-acetyl-phenylalanine (3)[b]	1-Cl	1.2	0.29
phenyllactate (4)[b]	1-Cl	0.968	0.526
mandelate (5)[b]	1-Cl	1.22	0.00207
methoxyphenylacetate (6)[b]	1-Cl	1.2	0.13

[a] K_S/K_R values are calculated from the association constants for the binding of the first guest to 1 as determined by ITC at 293 K in 2 mM aqueous MOPS buffer at pH 7.6. [b] K_S/K_R values are calculated from the association constants of the guest with 1-Cl determined with the competition CV assay. Solution conditions were 100 mM KCl in 10 mL of a 50% methanol 50% 100 mM aq MOPS buffer, $_s^s$pH = 7.5. [c] The p-value is a two-sided p-value that correlates to the null hypothesis that the binding constant of the S enantiomer is equal to the R- enantiomer.

■ DISCUSSION

A thorough understanding of the molecular recognition behavior of Ln(III)[15-MC-5] complexes is necessary for the development of the supramolecular host for separations, catalysis, materials design, or other practical applications. To determine the extent that Gd(III)[15-MC$_{Cu(II), L-pheHA}$-5] hosts discriminate between guests based on functional groups and chirality, we have investigated the inclusion of enantiomers of guests 2−6.

Differential binding of chiral guests by 1 is revealed in the crystal structures of the 1-S-2 and 1-R-2 inclusion complexes. Differential binding is evident in the hydrogen bonding network between 1, nitrate counterions, solvent, and the guests in the two structures. Particularly, hydrogen bonding interactions between the ammonium of 2 with heteroatoms in the MC ring are only observed with the S-enantiomer. On the basis of this associative
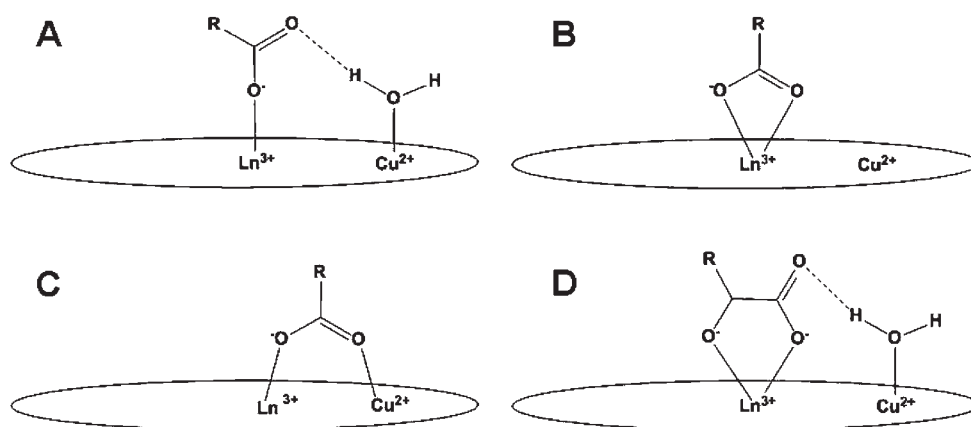
Figure 8. Illustration of the various binding modes for carboxylates bound to Ln(III)[15-MC-5] complexes. A–C have been observed crystallographically, while D is a proposed structure for α-hydroxycarboxlyates.

interaction, one would expect that *S*-**2** would bind more strongly to **1** in solution.

ITC revealed that in solution, the hydrophobic cavity of **1**-Cl exhibits a slight thermodynamic preference for the binding of the first *S*-**2** guest, with a K_S/K_R ratio of 1.6. A *t* test was performed to assess the statistical significance of this chiral discrimination, and p-values related to the null hypothesis that the binding constants for the *S*- and *R*-enantiomer are equal are displayed in Table 3. It was found that the observed selectivity between **1**-Cl and enantiomers of **2** was significant at the 5% confidence level.

Counterion effects in guest binding are known to influence guest binding to charged supramolecular hosts. Counterion effects with Ln(III)[15-MC-5] hosts have not been assessed previously in solution. In the solid state, the soft chloride anion is observed binding exclusively to Cu(II) ring metals on the hydrophilic face of the host or residing uncoordinated in the lattice. In contrast, nitrate can bind to either the hydrophilic or hydrophobic face and can bind to Cu(II) ring metals or the highly acidic Ln(III) central ion. Furthermore, nitrate can bind in a more stable bidentate coordination mode to the Ln(III) ion. For these reasons, it was hypothesized that nitrate might effectively compete with carboxylate guests for the Ln(III)[15-MC-5] host in solution whereas chloride might not pose an interference. To assess this quantitatively, the affinity of **1**-NO₃ for *S*- and *R*-**2** was measured (Table 1). Both **1**-Cl and **1**-NO₃ exhibit similar affinities for the guest **2**, demonstrating that nitrate does not have sufficiently strong interactions with host **1** in solution to perturb guest binding. Statistically significant enantioselective guest binding is also observed with host **1**-NO₃.

Though the crystal structures of the **1**-*R*-**2** and **1**-*S*-**2** complexes reveal differential binding in the solid state, enantioselectivity in solution is modest. Three distinctions account for this discrepancy. First, the associative hydrogen bonding interactions between the ammonium on *S*-**2** and **1** are likely quite weak in aqueous solution because of competition from the solvent. Thus, the formation of a hydrogen bond would be expected to generate only a small increase in the binding affinity. Second, the binding mode adopted by **2** in solution likely differs from that observed in the crystal structures, where **2** is bound monodentate through a carboxylate oxygen (Figure 8a). Importantly, the associative interactions between the ammonium on *S*-**2** and ring-heteroatoms on **1** are facilitated by the monodentate carboxylate coordination. However, this is an exceptional coordination mode

for a carboxylate guest encapsulated in the hydrophobic cavity and may be a result of the bidentate nitrate coordination to the Gd(III) on the hydrophilic face. Typically, crystal structures of Ln(III)[15-MC-5](carboxylate) complexes show encapsulated carboxylates binding bidentate to the central metal (Figure 8b) or adopting a bridging mode between the central Ln(III) and a Cu(II) ring metal (Figure 8c). For **2**, this bidentate binding mode would orient the ammonium of both enantiomers away from the MC face, preventing the chiral MC ring on **1** from discriminating between the different enantiomers. Therefore, it is likely that **2** binds bidentate in solution, which diminishes the observed enantioselectivity. Third, the binding strength of *S*- and *R*-**2** is rather weak. Therefore, any preference for a particular enantiomer could be moderated by the weak interaction with **1**. More strongly bound guests could reveal greater enantioselectivity.

The weak binding of **2** can be partially attributed to its zwitterionic charge state at neutral pH. Previous work has shown that **1** has association constants with zwitterions that are ~10 times less than a comparable −1 charged guest.[55] Thus we investigated the inclusion of guests **3**–**6** as they have a −1 charge at neutral pH and therefore were expected to bind more strongly to **1**. However, guests **3** and **6** bind quite weakly, with association constants of approximately 10^2 M⁻¹. Unfortunately, enantiomers of **3** or **6** are not discriminated by **1**, as no statistically significant selectivity is observed at the 5% confidence level (Table 3). Strong binding is observed with **4**. The association constants for *S*- and *R*-**4** are 2070 and 2140 M⁻¹, respectively. Again, no enantioselectivity is observed, suggesting the modest chiral discrimination does not exclusively arise from the weak binding strength.

Interestingly, the association constant between *S*-**5** and **1** is 22% greater than with *R*-**5**. This enantioselectivity cannot be attributed to how the guest is coordinated to the MC face because the enantiomers of **4** would be expected to bind in the same way. Instead, the chiral recognition likely arises from how the hydrophobic cavity recognizes the guest's side-chain. **4** has a phenyl chain while **5** has a benzyl chain. Likely the aromatic ring on *R*-**5** has a mild steric clash with a phenyl-side chain on **1**, resulting in weaker binding relative to *S*-**5**. The extra methylene carbon on *R*-**4** likely orients the aromatic ring so that this unfavorable interaction is avoided, and identical binding is observed for *R*-**4** and *S*-**4**.

The association constants of guests **2**–**6** with the hydrophobic cavity on **1** allows for comparison of how different guest

functionalities impact binding strength. Guests **2**−**4** are analogues of hydrocinnamate (**7**), while **5** and **6** are analogues of phenylacetate (**8**). The association constants of **7** and **8** with **1** were previously measured by ITC in an aqueous pH 7.6 solution at 298 K.[53] Despite the differences in the conditions, association constants for **7** and **8** determined by the CV competitive binding assay reproduced the corresponding ITC values adequately for K_{a1}, which is attributed to guest binding in the hydrophobic cavity. A similar correlation in the association constants for benzoate determined by the ITC and CV techniques was previously observed.[55] Given this general correlation between the ITC and CV measurements, we feel that approximate comparisons of values determined with the different techniques are acceptable for guests with disparate association constants. On the basis of the structure of the Ln(III)[15-MC$_{Cu(II), N, L-pheHA}$-5] hydrophobic cavity, one would expect that the introduction of hydrophilic functionalities on encapsulated guests could influence guest binding in two ways. First, guest binding could be weaker because of steric constraints or the enthalpic penalty of including a hydrophilic residue in a hydrophobic pocket. Second, guest affinity could increase because of favorable interactions between the hydrophilic MC face and the guest's hydrophilic functional groups.

The K_{a1} value determined by ITC between **1**-Cl and **7** at 298 K is 370 M^{-1}.[53] From the ΔH and ΔS values for the binding of **2**, association constants between **1**-Cl and **2** at 298 K are calculated to be 77 M^{-1} and 64 M^{-1} for the *S*- and *R*-enantiomers respectively. From these values, it is evident that the introduction of the ammonium group results in over a 4-fold decrease in the host−guest association constant. The lower affinity for **2** exhibited by **1** can be attributed in part to the guest's zwitterionic charge state, though unfavorable interactions between the ammonium group and the hydrophobic cavity likely contribute as well. Considering guest **3**, it is evident that the *N*-acetyl functionality similarly decreases K_a relative to the unsubstituted analogue, **7**. Presumably steric factors and unfavorable interactions between the hydrophilic *N*-acetyl group with the hydrophobic cavity cause this weak binding.

In contrast, the interaction between the hydroxy-substituted guest **4** and **1** is much stronger than that observed with guest **7**. Hydroxy-substituted **5** also has a strong interaction with **1** when compared to its unsubstituted analogue, **8**. This implies a strong associative interaction between the hydroxyl group on the α-carbon and the MC face. Crystal structures of carboxylates bound to **1** almost always show the carboxylate bound bidentate to Gd(III) (Figure 8b). This coordination mode orients the substituents on the α-carbon away from the MC face. The strong binding enhancement observed with the hydroxy-group suggests that **4** and **5** do not coordinate in this way. Instead, the guests likely adopt a bridging mode between a carboxylate oxygen atom and the oxygen off of the α-carbon, forming a five-membered chelate ring (Figure 8d). The hydroxyl-group likely undergoes a metal-assisted deprotonation in the hydrophobic cavity. A −2 charged guest would bind much more strongly to **1** than a −1 charged guest. It seems likely that **4** and **5** are deprotonated considering the magnitude of their binding constants. Unfortunately, crystal structures of **4** or **5** bound to **1** could not be obtained to confirm this conclusion. Interestingly, the reported binding constant of 12,800 ± 300 M^{-1} for coumarin 343 (**9**) to Eu^{3+}[15-MC$_{Cu(II), L-pheHA}$-5] is also much greater than the values typically observed for simple carboxylates.[54] While **9** has significant structural differences with **4** and **5** and the solution

conditions are different between the measurements, the guests can all form chelate rings with a Ln(III) central metal through a carboxylate oxygen and another donor oxygen possessing significant electron density. On **9**, this oxygen comes from a carbonyl and not the alkoxide seen with **4** and **5**. However, resonance could place significant electron density at the carbonyl oxygen and enhance binding. Thus, self-consistent binding constants on the order of 10^3−10^4 have been observed for hydrophobic guests that coordinate through two formally negatively charged oxygen atoms to a Ln(III)[15-MC$_{Cu(II), L-pheHA}$-5] host.

Metal-assisted deprotonation of guests **4** and **5** is further supported by the weak binding of **6**. Replacing the alcohol group on **5** with the methoxy group of **6** decreases the association constant with **1** more than 20-fold. While the ether is sterically bulkier than the alcohol and is a weaker electron donor, these differences are not likely to account for the 20 times smaller K_a. The difference in charge between the −2 charged alkoxide **5** and the −1 charged **6** is a better explanation for the discrepancy. Interestingly, **6** displays a smaller association constant with **1** than **8**, further demonstrating that neutral hydrophilic groups on the α-carbon decrease the binding affinity of carboxylate guests. If the association constants of benzoate (690 ± 120 M^{-1}), ferrocene carboxylate (1040 ± 100 M^{-1}), and ferrocenium carboxylate (100 ± 30 M^{-1}) with **1** are also considered,[55] a trend in guest binding strength emerges. Simple −1 charged carboxylates possess association constants on the order of 10^2−10^3 M^{-1}. Association constants of 10^1 to 10^2 M^{-1} are observed for zwitterionic carboxylates and values of 10^3−10^4 have been measured for carboxylates substituted with a highly electron rich donor oxygen at the α-carbon.

■ CONCLUSION

Differential binding of enantiomers was demonstrated by host **1** in the solid state with α-phenylalanine enantiomers. In solution, modest enantioselectivity was observed with certain guests. Furthermore, disparate association constants for carboxylate guests were measured based on the substitution of the α-carbon. Three significant conclusions can be drawn from these results. First, Ln(III)[15-MC-5] complexes are capable of, albeit weak, enantioselective guest recognition. Second, guest binding constants can be varied by 2 orders of magnitude based on the substitution of the carboxylate at the α-carbon. This selectivity for guests based on their chemical functionalities or chirality has not been demonstrated previously with this class of supramolecular hosts and has broad implications for the development Ln(III)[15-MC-5] complexes as supramolecular catalysts, in separations, or as building blocks for chiral solids. Notably, the structural versatility of the [15-MC-5] platform could provide the means for enhancing guest selectivity through changes to the ligand side chains, central metal, or ring metal. Third, the significant binding enhancement observed with guests **4** and **5** is suggestive of a metal-assisted deprotonation of the hydroxyl group. This observation reveals the strong Lewis-acidity of Ln(III)[15-MC-5] complexes, which could potentially find utility in facilitating chemical transformations.

■ ASSOCIATED CONTENT

ⓢ **Supporting Information.** Additional thermodynamic tables, crystallographic information files (CIFs), and crystallographic

4839

dx.doi.org/10.1021/ic102579t |*Inorg. Chem.* 2011, 50, 4832–4841

tables. This material is available free of charge via the Internet at http://pubs.acs.org.

■ AUTHOR INFORMATION

Corresponding Author
*E-mail: vlpec@umich.edu.

■ ACKNOWLEDGMENT

■ REFERENCES

(1) Lehn, J.-M. *Supramolecular Chemistry: Concepts and Perspectives*; VCH Verlagsgesellschaft: New York, 1995.

(2) Steed, J. W.; Atwood, J. L. *Supramolecular Chemistry*; John Wiley & Sons, Ltd: West Sussex, 2000.

(3) Hof, F.; Craig, S. L.; Nuckolls, C.; Rebek, J. J. *Angew. Chem., Int. Ed.* **2002**, *41*, 1488.

(4) Yoshizawa, M.; Klosterman, J. K.; Fujita, M. *Angew. Chem., Int. Ed.* **2009**, *48*, 3418.

(5) Fiedler, D.; Leung, D. H.; Bergman, R. G.; Raymond, K. N. *Acc. Chem. Res.* **2004**, *38*, 349.

(6) Pluth, M. D.; Bergman, R. G.; Raymond, K. N. *Acc. Chem. Res.* **2009**, *42*, 1650.

(7) Laughrey, Z.; Gibb, B. C. *Chem. Soc. Rev.* **2011**, *40*, 363.

(8) *Supramolecular Chirality*; Crego-Calama, M., Reinhoudt, D. N., Eds.; Springer: Berlin, Germany, 2006; Vol. 265.

(9) Easton, C. J.; Lincoln, S. F. *Chem. Soc. Rev.* **1996**, 163.

(10) Hambury, G. A.; Borovkov, V. V.; Inoue, Y. *Chem. Rev.* **2008**, *108*, 1.

(11) Sumna, A. *Chem. Soc. Rev.* **2010**, *39*, 4274.

(12) *Supramolecular Catalysis*; Leeuwen, P. W. N. M. v., Ed.; Wiley-VCH Verlag GmbH & Co. KGaA: Weinheim, Germany, 2008.

(13) Schmidtchen, F. P. *Chem. Soc. Rev.* **2010**, *39*, 3916.

(14) Baron, R.; Setny, P.; McCammon, J. A. *J. Am. Chem. Soc.* **2010**, *132*, 12091.

(15) Ballester, P. *Chem. Soc. Rev.* **2010**, *39*, 3810.

(16) O'Neil, E. J.; Smith, B. D. *Coord. Chem. Rev.* **2006**, *250*, 3068.

(17) Lozan, V.; Buchholz, A.; Plass, W.; Kersting, B. *Chem.—Eur. J.* **2007**, *13*, 7305.

(18) Dalgarno, S. J.; Power, N. P.; Atwood, J. L. *Coord. Chem. Rev.* **2008**, *252*, 825.

(19) Parker, R. J.; Spiccia, L.; Moubaraki, B.; Murray, K. S.; Hockless, D. C. R.; Rae, A. D.; Willis, A. C. *Inorg. Chem.* **2002**, *41*, 2489.

(20) Damsyik, A.; Lincoln, S. F.; Wainwright, K. P. *Inorg. Chem.* **2006**, *45*, 9834.

(21) Frischmann, P. D.; Facey, G. A.; Ghi, P. Y.; Gallant, A. J.; Bryce, D. L.; Lelj, F.; MacLachlan, M. J. *J. Am. Chem. Soc.* **2010**, *132*, 3893.

(22) Armentano, D.; Marino, N.; Mastropietro, T. F.; Martínez-Lillo, J.; Cano, J.; Julve, M.; Lloret, F.; De Munno, G. *Inorg. Chem.* **2008**, *47*, 10229.

(23) Jones, L. F.; Kilner, C. A.; Halcrow, M. A. *Chem.—Eur. J.* **2009**, *15*, 4667.

(24) Mezei, G.; Zaleski, C. M.; Pecoraro, V. L. *Chem. Rev.* **2007**, *107*, 4933.

(25) Lah, M. S.; Kirk, M. L.; Hatfield, W.; Pecoraro, V. L. *J. Chem. Soc., Chem. Commun.* **1989**, 1606.

(26) Lah, M. S.; Pecoraro, V. L. *J. Am. Chem. Soc.* **1989**, *111*, 7258.

(27) Lah, M. S.; Pecoraro, V. L. *Comments Inorg. Chem.* **1990**, *11*, 59.

(28) Lah, M. S.; Pecoraro, V. L. *Inorg. Chem.* **1991**, *30*, 878.

(29) Gibney, B. R.; Kessissoglou, D. P.; Kampf, J. W.; Pecoraro, V. L. *Inorg. Chem.* **1994**, *33*, 4840.

(30) Stemmler, A. J.; Kampf, J. W.; Pecoraro, V. L. *Inorg. Chem.* **1995**, *34*, 2271.

(31) Pecoraro, V. L.; Stemmler, A. J.; Gibney, B. R.; Bodwin, J. J.; Wang, H.; Kampf, J. W.; Barwinski, A. In *Progress in Inorganic Chemistry*; Karlin, K. D., Ed.; John Wiley and Sons, Inc.: New York, 1997; Vol. 45, p 83.

(32) Psomas, G.; Stemmler, A. J.; Dendrinou-Samara, C.; Bodwin, J. J.; Scheider, M.; Alexiou, M.; Kampf, J. W.; Kessissoglou, D. P.; Pecoraro, V. L. *Inorg. Chem.* **2001**, *40*, 1562.

(33) Kessissoglou, D. P.; Bodwin, J. J.; Kampf, J. W.; Dendrinou-Samara, C.; Pecoraro, V. L. *Inorg. Chim. Acta* **2002**, *331*, 73.

(34) Dendrinou-Samara, C.; Psomas, G.; Iordanidis, L.; Tangoulis, V.; Kessissoglou, D. P. *Chem.—Eur. J.* **2001**, *7*, 5041.

(35) Mezei, G.; Baran, P.; Raptis, R. G. *Angew. Chem., Int. Ed.* **2004**, *43*, 574.

(36) Dendrinou-Samara, C.; Alevizopoulou, L.; Iordanidis, L.; Samaras, E.; Kessissoglou, D. P. *J. Inorg. Biochem.* **2002**, *89*, 89.

(37) Emerich, B.; Smith, M.; Zeller, M.; Zaleski, C. M. *J. Chem. Crystallogr.* **2010**, *40*, 769.

(38) Boron, T. T., III; Kampf, J. W.; Pecoraro, V. L. *Inorg. Chem.* **2010**, *49*, 9104.

(39) Tegoni, M.; Ferretti, L.; Sansone, F.; Remelli, M.; Bertolasi, V.; Dallavalle, F. *Chem.—Eur. J.* **2007**, *13*, 1300.

(40) Saalfrank, R. W.; Low, N.; Kareth, S.; Seitz, V.; Hampel, F.; Stalke, D.; Teichert, M. *Angew. Chem., Int. Ed.* **1998**, *37*, 172.

(41) Bodwin, J. J.; Pecoraro, V. L. *Inorg. Chem.* **2000**, *39*, 3435.

(42) Bodwin, J. J.; Cutland, A. D.; Malkani, R. G.; Pecoraro, V. L. *Coord. Chem. Rev.* **2001**, *216—217*, 489.

(43) Pecoraro, V. L.; Bodwin, J. J.; Cutland, A. D. *J. Solid State Chem.* **2000**, *152*, 68.

(44) Stemmler, A. J.; Kampf, J. W.; Pecoraro, V. L. *Angew. Chem., Int. Ed. Engl.* **1996**, *35*, 2841.

(45) Stemmler, A. J.; Kampf, J. W.; Kirk, M. L.; Atasi, B. H.; Pecoraro, V. L. *Inorg. Chem.* **1999**, *38*, 2807.

(46) Seda, S. H.; Janczak, J.; Lisowski, J. *Inorg. Chem. Commun.* **2006**, *9*, 792.

(47) Seda, S. H.; Janczak, J.; Lisowski, J. *Eur. J. Inorg. Chem.* **2007**, 3015.

(48) Stemmler, A. J.; Barwinski, A.; Baldwin, M. J.; Young, V.; Pecoraro, V. L. *J. Am. Chem. Soc.* **1996**, *118*, 11962.

(49) Cutland, A. D.; Malkani, R. G.; Kampf, J. W.; Pecoraro, V. L. *Angew. Chem., Int. Ed.* **2000**, *39*, 2689.

(50) Cutland-Van Noord, A. C.; Kampf, J. W.; Pecoraro, V. L. *Angew. Chem., Int. Ed.* **2002**, *41*, 4667.

(51) Zaleski, C. M.; Cutland-Van Noord, A. D.; Kampf, J. W.; Pecoraro, V. L. *Cryst. Growth Des.* **2007**, *7*, 1098.

(52) Zaleski, C. M.; Depperman, E. C.; Kampf, J. W.; Kirk, M. L.; Pecoraro, V. L. *Inorg. Chem.* **2006**, *45*, 10022.

(53) Lim, C.-S.; Kampf, J. W.; Pecoraro, V. L. *Inorg. Chem.* **2009**, *48*, 5224.

(54) Tegoni, M.; Tropiano, M.; Marchio, L. *Dalton Trans.* **2009**, 6705.

(55) Jankolovits, J.; Kampf, J. W.; Maldonado, S.; Pecoraro, V. L. *Chem.—Eur. J.* **2010**, *16*, 6786.

(56) Lim, C. S.; Jankolovits, J.; Kampf, J. W.; Pecoraro, V. L. *Chem. Asian J.* **2010**, *5*, 46.

(57) Cutland, A. D.; Halfen, J. A.; Kampf, J. W.; Pecoraro, V. L. *J. Am. Chem. Soc.* **2001**, *123*, 6211.

(58) Lim, C.-S.; Noord, A. C. V.; Kampf, J. W.; Pecoraro, V. L. *Eur. J. Inorg. Chem.* **2007**, 1347.

(59) Mezei, G.; Kampf, J. W.; Pan, S.; Poeppelmeier, K. R.; Watkins, B.; Pecoraro, V. L. *Chem. Commun.* **2007**, *11*, 1148.

(60) Jankolovits, J.; Lim, C.-S.; Kampf, J. W.; Pecoraro, V. L. *Z. Naturforsch.* **2010**, *65b*, 263.

(61) Dallavalle, F.; Remelli, M.; Sansone, F.; Bacco, D.; Tegoni, M. *Inorg. Chem.* **2010**, *49*, 1761.

4840

dx.doi.org/10.1021/ic102579t |*Inorg. Chem.* 2011, 50, 4832–4841

(62) Tegoni, M.; Furlotti, M.; Tropiano, M.; Lim, C.-S.; Pecoraro, V. L. *Inorg. Chem.* **2010**, *49*, 5190.

(63) Castellano, R. K.; Kim, B. H.; J. Rebek, J. *J. Am. Chem. Soc.* **1997**, *119*, 12671.

(64) Siracusa, L.; Hurley, F. M.; Dresen, S.; Lawless, L. J.; Pérez-Payán, M. N.; Davis, A. P. *Org. Lett.* **2002**, *4*, 4639.

(65) Rivera, J. M.; Martin, T.; J. Rebek, J. *Science* **1998**, *279*, 1021.

(66) Kuberski, B.; Szumna, A. *Chem. Commun.* **2009**, *2009*, 1959.

(67) Fiedler, D.; Leung, D. H.; Bergman, R. G.; Raymond, K. N. *J. Am. Chem. Soc.* **2004**, *126*, 3674.

(68) Brumaghim, J. L.; Michels, M.; Raymond, K. N. *Eur. J. Org. Chem.* **2004**, *22*, 4552.

(69) Nuckolls, C.; Hof, F.; Martín, T.; Rebek, J., Jr. *J. Am. Chem. Soc.* **1999**, *121*, 10281.

(70) Rivera, J. M.; Martín, T.; Rebek, J., Jr. *J. Am. Chem. Soc.* **2001**, *123*, 5213.

(71) Ali, L. A.; Cox, A.; Kemp, T. J. *J. Chem. Soc., Dalton Trans.* **1973**, 1468.

(72) Canals, I.; Portal, J. A.; Bosch, E.; Roses, M. *Anal. Chem.* **2000**, *72*, 1802.

(73) Rived, F.; Rosés, M.; Bosch, E. *Anal. Chim. Acta* **1998**, *374*, 309.

(74) Perrin, D. D.; Dempsey, B. *Buffers for pH and Metal ion control*; Chapman and Hall: London, U.K., 1979.

(75) Canals, I.; Oumada, F. Z.; Oumada, M. Z.; Roses, M.; Bosch, E. *J. Chromatogr., A.* **2001**, *911*, 191.

(76) Azab, H. A.; Ahmed, I. T.; Mahmoud, M. R. *J. Chem. Eng. Data* **1995**, *40*, 523.

(77) Azab, H. A.; Orabi, A. S.; El-Salam, E. T. A. *J. Chem. Eng. Data* **1998**, *43*, 703.

(78) *SAINT Plus*, v. 7.60A; Bruker Analytical X-ray: Madison, WI, 2008.

(79) Sheldrick, G. M. *SADABS, Program for Empirical Absorbtion Correction of Area Detector Data*, v. 2008/1; University of Göttingen: Göttingen, Germany, 2008.

(80) Sheldrick, G. M. *SHELXTL*, v. 2008/4; Bruker Analytical X-ray: Madison, WI, 2008.

4841

dx.doi.org/10.1021/ic102579t |*Inorg. Chem.* 2011, 50, 4832–4841